crystals

MDPI

Article

Rare earth ions doped $Y_{2.95}R_{0.05}MgAl_3SiO_{12}$ (R = Yb, Y, Dy, Eu, Sm) garnet-type microwave ceramics for 5G application

Zijun Ye[a], Yu Jiang[a], Minmin Mao[a,*], Zhiyu Xiu[a], Mengjiao Chi[a], Guofa Wu[a], Bing Liu[a], Dawei Wang[b,*], Bin Yang[c], Kaixin Song[a,*]

[a]College of Electronics Information, Hangzhou Dianzi University, Hangzhou, 310018, China
[b]Functional Materials and Acousto-Optic Instruments Institute, School of Instrumentation Science and Engineering, Harbin Institute of Technology, Harbin 150080, China
[c]Faculty of Science and Engineering, University of Chester, Chester CH1 4BJ, UK
* Correspondence: mmm@hdu.edu.cn; kxsong@hdu.edu.cn; wangdawei102@gmail.com

Abstract: In this work, $Y_{2.95}R_{0.05}MgAl_3SiO_{12}$ (R=Yb, Y, Dy, Eu, Sm) microwave single-phase dielectric ceramics were successfully prepared via conventional ceramic technology by doping a series of rare earth elements with different ionic radius (Yb, Y, Dy, Eu, Sm) for the first time. The effects of A site occupied by rare earth elements on the microwave dielectric properties of $Y_{2.95}R_{0.05}MgAl_3SiO_{12}$ were studied by crystal structure refinement, scanning electron microscope (SEM), bond valence theory, P-V-L theory and infrared reflection spectroscopy. It was found that the ionicity of Y-O bond, the lattice energy, the bond energy and bond valance of $Al_{(Tet)}$-O bond had important effects on microwave dielectric properties. Particularly, the optimum microwave dielectric properties were obtained for $Y_{2.95}Dy_{0.05}MgAl_3SiO_{12}$ sintered at 1575 °C for 6 h, with ε_r = 9.68, $Q\times f$ = 68,866 GHz, and τ_f = -35.8 ppm/°C, displaying its potential prospect in the 5G communication.

Keywords: Garnet; Microwave dielectric properties; P-V-L theory; Infrared reflection spectroscopy

Citation: Lastname, F.; Lastname, F.; Last-name, F. Title. *Crystals* **2021**, *11*, x. https://doi.org/10.3390/xxxxx

Received: date
Accepted: date
Published: date

1. Introduction

With the rapid development of communication frequency bands to millimeter-wave band, the properties of microwave dielectric ceramic materials used in communication equipments are required to have the following dielectric properties:

(1) low ε_r to get low delay in the signal transmission process, (2) the ultra-high $Q\times f$ value reduces the transmission loss and (3) near-zero temperature coefficient (τ_f) can improve the device stability in different environments, applied in resonators, antennas, filters and 5G base stations, etc [1-6].

In low dielectric constant material systems, $Y_3Al_5O_{12}$ garnet has attracted extensive research due to its low ε_r and high $Q\times f$ value in 5G communication system[7]. Figure 1 shows the $Q\times f$ values of the various types of garnet-type microwave dielectric ceramics, including Vanadate Garnet, Aluminate Garnet, etc [8-24]. It is clear that the $Q\times f$ value of aluminate garnet is much higher than that of others. Aluminate garnet has the formula of $Y_3Al_5O_{12}$ (YAG), in which three Y^{3+} ions occupy A-site dodecahedral, two $Al_{(Oct)}^{3+}$ ions occupy B-site octahedral, and three $Al_{(Tet)}^{3+}$ ions occupy C-site tetrahedral. The $Q\times f$ of $Y_3Al_5O_{12}$ microwave ceramics was initially reported to be as high as 440,000 GHz [25]. Later, Jin et al.[12] reported excellent microwave dielectric properties of ε_r = 10.8, $Q\times f$ = 213,400 GHz, τ_f = -30 ppm/°C for $Y_3Al_5O_{12}$ ceramic, which was pressed under 200MPa by cold isostatic pressing technology and sintered at 1750 °C for 5h in a vacuum environment. Zhou et al.[15] synthesized $Y_3Al_{4.97}Mg_{0.03}O_{11.985}$ microwave ceramics by replacing $Al_{(Oct)}^{3+}$ with Mg^{2+}, and sintering at 1700°C for 12h, which showed excellent microwave dielectric properties: ε_r = 10.9, $Q\times f$ = 218,168 GHz, τ_f = -30 ppm/°C. And then, non-stoichiometric YAG ceramics ($Y_{3.03}Al_5O_{12}$) were further synthesized at 1750 °C for 12, showing good microwave

dielectric properties: ε_r = 11.2, $Q \times f$ = 236,936 GHz, τ_f = -35.9 ppm/°C [16]. However, the sintering temperature of YAG ceramics is too high (> 1700 °C), which does not conform to the concept of low carbon and environmental protection. In order to solve the problems of high sintering temperature and large τ_f, a lot of research has been carried out. Zhang et al.[14] reported that the sintering temperature of YAG ceramics was reduced from 1700 °C to 1360 °C by using LiF as additive, showing $Q \times f$ = 89,810 GHz, ε_r = 10.63 and τ_f = -51.4 ppm/°C. Peng et al.[26] reported a near-zero τ_f value (+7 ppm/°C) for Ca^{2+} and Ti^{4+} co-doped $Ca_{1.5}Y_{1.5}Al_{3.5}Ti_{1.5}O_{12}$ ceramics, with ε_r = 32.6 and $Q \times f$ = 45,200 GHz.

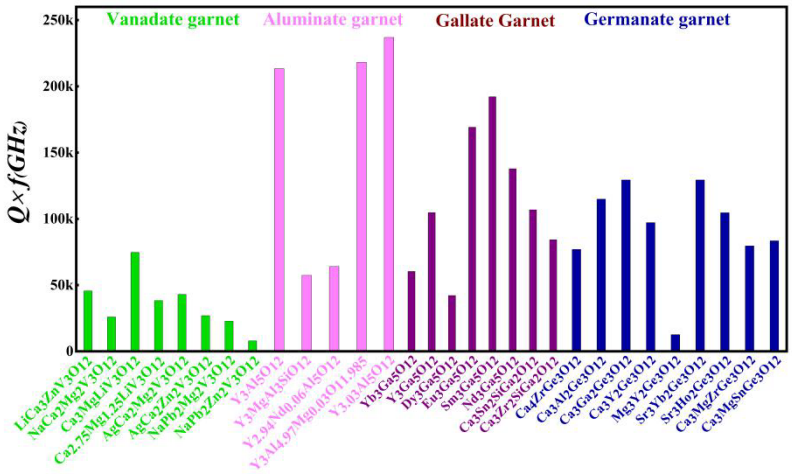

Figure 1. $Q \times f$ values of typical garnet-type microwave dielectric ceramics.

Previous reports showed that MgO-SiO_2 liquid phase was formed in $Y_3Al_5O_{12}$ garnet ceramics with MgO and SiO_2 as sintering aids, which improved the densification rate of ceramics [27]. Compared with YAG ceramics, the $Y_3MgAl_3SiO_{12}$ ceramics had been formed by doping Mg^{2+} at B-site octahedrons and Si^{4+} at C-site tetrahedrons of YAG, which reduced the sintering temperature from 1670 °C to 1550 °C and exhibited good microwave dielectric performances of ε_r = 10.1, $Q \times f$ = 57,340 GHz and τ_f = -32 ppm/°C [13,28,29]. The τ_f of $Y_3MgAl_3SiO_{12}$ was further tuned to near-zero value (+5.2 ppm/°C) by forming composites with 0.2TiO_2 [30]. However, the modification of A-site dodecahedrons for garnet ceramics was the subject of very little research. Herein, we designed a scheme of A site ionic substitution for Y element at $Y_3MgAl_3SiO_{12}$ ceramics using a series of rare earth elements with different ionic radius (Yb, Y, Dy, Eu, Sm). The microwave dielectric properties of $Y_{2.95}R_{0.05}MgAl_3SiO_{12}$ (R=Yb, Y, Dy, Eu, Sm) ceramic were well discussed by crystal structure refinement, bond valence theory, P-V-L theory and infrared reflectance spectrum.

2. Experimental process

$Y_{2.95}R_{0.05}MgAl_3SiO_{12}$ (R=Yb, Y, Dy, Eu, Sm) ceramics were composited by raw materials of Yb_2O_3 (Shanghai Aladdin Reagent Co., Ltd., 99.99%), Y_2O_3 (Shanghai Aladdin Reagent Co., Ltd., 99.99%), Dy_2O_3 (Shanghai Aladdin Reagent Co., Ltd., 99.99%), Eu_2O_3 (Shanghai Aladdin Reagent Co., Ltd., 99.99%), Sm_2O_3 (Shanghai Aladdin Reagent Co., Ltd., 99.99%), MgO (Shanghai Aladdin Reagent Co., Ltd., 99.99%), Al_2O_3 (Shanghai Aladdin Reagent Co., Ltd., 99.99%), and SiO_2 (Shanghai Aladdin Reagent Co., Ltd., 99.99%). Raw materials were weighed according to the stoichiometric ratio and planetarily ball-milled for 12 h in solvent ethanol. The speed for milling was 240 r/min. The mixed slurries were dried at 80°C, and then the dried powders were calcined at 1400°C for 4 h. The calcined powder was re-milled and mixed uniformly with 5wt% organic binders (polyvinyl alcohol). The granulated powder was sieved by a 60-mesh sieve and pressed into cylindrical green pellets with a diameter of 12 mm and a height of ~7 mm. The green pellets

were first fired at 800 °C for 4 h to remove binder, and then sintered at 1500 °C -1650 °C for 6 h.

The crystal structure was identified by X-ray powder diffraction (XRD) (Shimadzu, Kyoto, Japan) using Cu Kα radiationat the range of 2θ from 10° to 80° with a step size of 0.02°. The GSAS software was used to analyze the crystal structure parameters of X-ray diffraction data [31,32]. The microstructure of the sintered samples were observed by the field emission scanning electron microscope (Sigma 300, ZEISS). The Archimedes method was used to determine the bulk density. The infrared reflectance spectra were recorded using the Bruker IFS 66v beam line of the Hefei National Synchrotron Radiation Laboratory. The surfaces of the samples for FIR measurements was polished. Microwave dielectric properties were measured in $TE_{01\delta}$ mode using the resonant cavity method. The Keysight (N5234B) vector network analyzer was used for evaluating the Q×f values and ε_r. The τ_f value was calculated by the following formual [33]:

$$\tau_f = \frac{f_2 - f_1}{f_1 \times (T_2 - T_1)} \times 10^6 (ppm/℃) \quad (1)$$

where f_1 and f_2 were the resonant frequency at 25 and 85 °C, respectively.

3. Results and discussion

The XRD patterns of $Y_{2.95}R_{0.05}MgAl_3SiO_{12}$ (R=Yb, Y, Dy, Eu, Sm) ceramics are displayed in Figure 2 . The diffraction peaks of all samples match well with the YAG structure (PDF No.88-2047), indicating the formation of garnet solid solution. It can be clearly seen that the diffraction peaks move to lower 2θ angle with the increase of R ionic radius (Yb^{3+} ~ 0.985 Å, Y^{3+} ~ 1.019 Å, Dy^{3+} ~ 1.027 Å, Eu^{3+} ~ 1.066 Å, Sm^{3+} ~ 1.079 Å) from magnified spectra in Figure 2(b). The XRD data of $Y_{2.95}R_{0.05}MgAl_3SiO_{12}$ ceramics are analyzed by Rietveld method, which are shown in Figure S2(a-e). Table 1 lists the detailed refined parameters. Lower Rietveld discrepancy factors (R_{wp}~9%, R_p~7%, χ^2~4) are obtained, suggesting the refinement results are reliable. The unit cell volume of $Y_{2.95}R_{0.05}MgAl_3SiO_{12}$ ceramics increases slightly with the increasing of R ionic radius, which is consistent with the diffraction peaks shift toward lower 2θ direction. The crystal structure schematic of $Y_{2.95}R_{0.05}MgAl_3SiO_{12}$ ceramics is given in Figure S1(f).

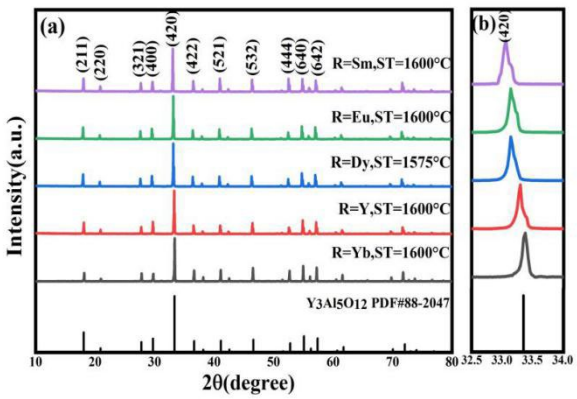

Figure 2. (a) XRD patterns of $Y_{2.95}R_{0.05}MgAl_3SiO_{12}$(R=Yb, Y, Dy, Eu, Sm) ceramic samples; (b) magnified XRD spectra.

Table 1 The crystallographic data from Rietveld refinement for $Y_{2.95}R_{0.05}MgAl_3SiO_{12}$ ceramics.

R	Yb	Y	Dy	Eu	Sm

Crystal system	cubic				
Space group	Ia-3d				
Z	8				
a=b=c(Å)	12.0482	12.0499	12.0529	12.0589	12.0668
$\alpha=\beta=\gamma(°)$	90				
$V_{cell}(Å^3)$	1749.121	1749.607	1750.103	1750.623	1751.009
Calc.density(g/cm^3)	4.602	4.357	4.538	4.527	4.417
R_{wp}(%)	9.17	10.5	9.8	10.1	9.8
R_p(%)	6.34	7.38	8.37	8.87	6.5
χ^2	4.36	4.35	2.65	3.06	2.64
Y/R-O (Å)	2.2932	2.3224	2.3002	2.3106	2.3329
	2.4466	2.4770	2.4782	2.4796	2.4865
$(Al_{(Oct)}/Mg)$-O (Å)	2.0038	1.9881	2.0062	1.9894	1.9649
$(Al_{(Tet)}/Si)$-O (Å)	1.7355	1.7257	1.7352	1.7387	1.7528

The SEM images of $Y_{2.95}R_{0.05}MgAl_3SiO_{12}$ (R=Yb, Y, Dy, Eu, Sm) ceramics sintered at optimal sintering temperature (Yb-1600°C, Y-1600°C, Dy-1575°C, Eu-1600°C, Sm-1600°C) are shown in Figure 3(a-e). All sintered ceramics are dense except for Sm-doped ceramics which have obvious voids. The grain size distribution of each sample is shown in Figure S2 (Supporting Information), and the average grain size is plotted in Figure 3(f). Among the rare earth elements in this study, $Y_{2.95}Dy_{0.05}MgAl_3SiO_{12}$ ceramics have the largest average grain size, indicating that Dy^{3+} doping is conducive to the densification and growth of ceramics.

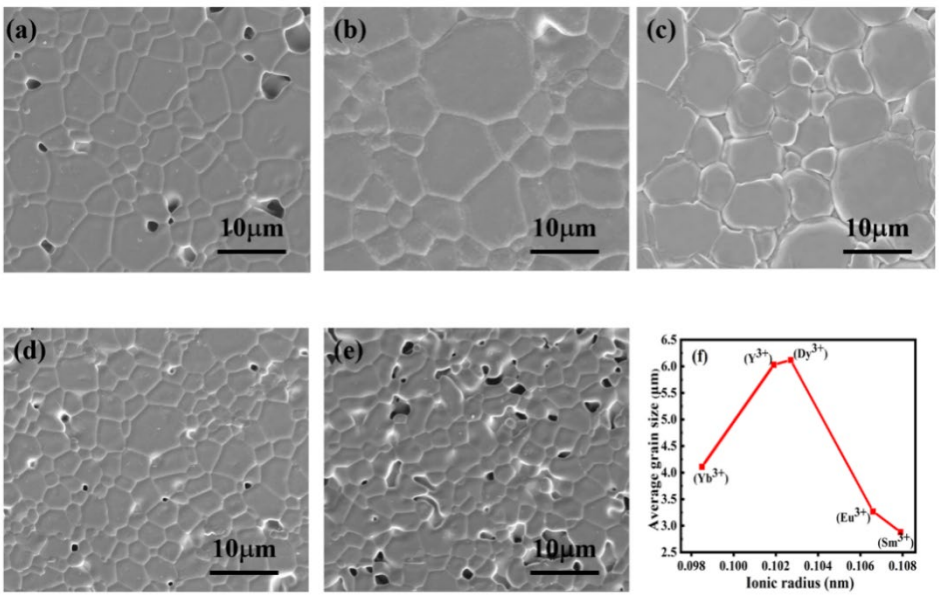

Figure 3. SEM images of $Y_{2.95}R_{0.05}MgAl_3SiO_{12}$ ceramics: (a) Yb; (b) Y; (c) Dy; (d) Eu; (e) Sm; (f) the average grain size.

Figure 4 exhibits the microwave dielectric properties of $Y_{2.95}R_{0.05}MgAl_3SiO_{12}$ (R=Yb, Y, Dy, Eu, Sm) ceramics sintered at the optimal temperature. ε_r shows a gradual increasing trend except R=Dy, which has a lower ε_r value of 9.68. The $Q\times f$ value is in the range of 47,000 GHz ~ 70,000 GHz, which is consistent with the trend of relative density (ρ_r). τ_f is between -38.7ppm/°C and -28.6ppm/°C. It is widely known that the microwave dielectric properties are dependent on both extrinsic (second phase, density and grain size, etc.) and intrinsic (lattice vibration) factors[34]. The relative density of $Y_{2.95}R_{0.05}MgAl_3SiO_{12}$ ceramic sintered at the optimal sintering temperature is high (ρ_r > 94%), and no secondary phase was detected. Therefore, the intrinsic factors, such as crystal structure and chemical bonds, play a decisive role on the dielectric properties. Herein, the relationship between the microwave dielectric properties and internal factors of $Y_{2.95}R_{0.05}MgAl_3SiO_{12}$ ceramics is discussed by P-V-L theory. The detailed calculation methods are included in the Supporting Information.

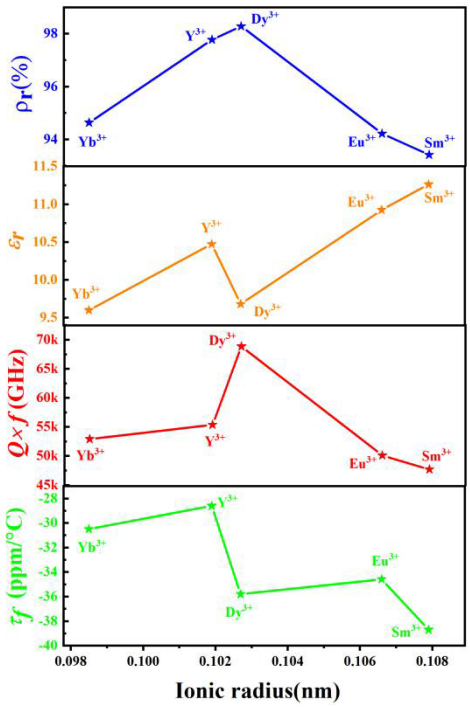

Figure 4. Microwave dielectric properties and ρ_r of $Y_{2.95}R_{0.05}MgAl_3SiO_{12}$ ceramics.

In general, the measured permittivity (ε_r) is related to the bond ionicity (f_i). The calculated results of f_i are listed in Table S1 (Supporting Information). In addition, the theoretical permittivity (ε_{theo}) of $Y_{2.95}R_{0.05}MgAl_3SiO_{12}$ ceramics can be calculated by the Clausius-Mosotti equations (2) and (3) [35-36]:

$$\varepsilon_{theo} = \frac{3}{1-b\alpha/V_m} - 2 \quad (2)$$

$$V_m = \frac{V_{cell}}{Z} \quad (3)$$

Besides, the corrected dielectric constant (ε_c) by porosity (P) can be calculated by equations (5) and (6) [37]:

$$P = 1 - \rho_r \quad (4)$$

$$\varepsilon_c = \varepsilon_r(1 + 1.5P) \quad (5)$$

As shown in Figure 5(a), the ε_r is consistent with the changing trend of ε_{theo}, ε_c and the average bond ionicity (Δf_i). The average ionicity properties of Y-O, $Al_{(Oct)}$-O and $Al_{(Tet)}$-O bonds of $Y_{2.95}R_{0.05}MgAl_3SiO_{12}$ (R=Yb, Y, Dy, Eu, Sm) are given in Figure 5(b), severally. The maximum value of f_i is 94.91% for Y-O bond, indicating the Y-O bond plays a leading role in affecting the ε_r value of $Y_{2.95}R_{0.05}MgAl_3SiO_{12}$ ceramics.

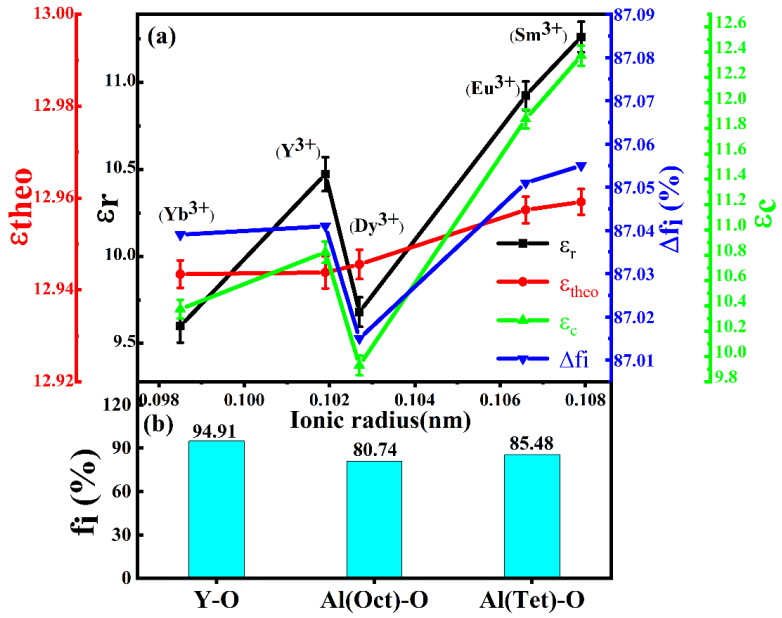

Figure 5. (a) ε_r, ε_{theo}, ε_c and Δf_i of $Y_{2.95}R_{0.05}MgAl_3SiO_{12}$ ceramics; (b) The average f_i of three types of bonds.

Lattice vibration of microwave dielectric ceramics has great influence on dielectric loss. The lattice energy of chemical bonds of microwave dielectric ceramics can effectively evaluate the lattice vibration of ceramics [38]. Therefore, we can use average lattice energy (U) value to predict the $Q \times f$ values and the calculation results of average lattice energy (U) value are listed in Table S2. The average lattice energy (U), grain size and $Q \times f$ values of $Y_{2.95}R_{0.05}MgAl_3SiO_{12}$ ceramics are shown in Figure 6(a). It can be seen that the average lattice energy (U) is consistent with the trend of $Q \times f$ values of $Y_{2.95}R_{0.05}MgAl_3SiO_{12}$ ceramics, suggesting the average lattice energy (U) is an important factor affecting $Q \times f$ values of $Y_{2.95}R_{0.05}MgAl_3SiO_{12}$ ceramics. Figure 6(b) shows the average U of Y-O bond, $Al_{(Oct)}$-O bond and $Al_{(Tet)}$-O bond in $Y_{2.95}R_{0.05}MgAl_3SiO_{12}$ ceramics ($Al_{(Tet)}$-O (33533kJ/mol)> Y-O(22143kJ/mol) > $Al_{(Oct)}$-O (21989kJ/mol)), which indicates that the $Al_{(Tet)}$-O bond plays a dominated role for the $Q \times f$ value. In addition, a larger average grain size shows fewer grain boundaries, which means higher $Q \times f$ values [39].

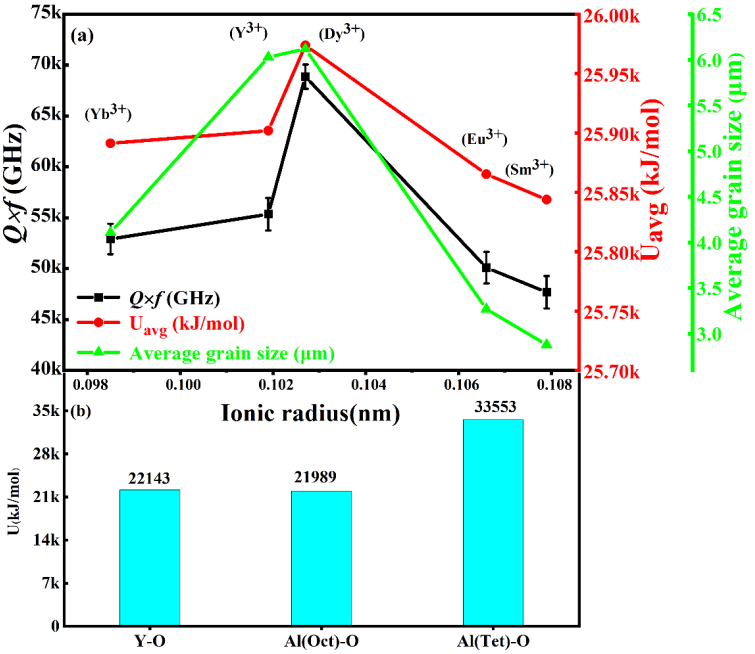

Figure 6. (a) *Q*×*f*, average lattice energy and average grain size of $Y_{2.95}R_{0.05}MgAl_3SiO_{12}$ ceramics; (b) The average U value of three types of bonds.

The temperature coefficient of resonance frequency (τ_f) is related to bond valence (V_{ij}) and bond energy (E). Bond energy (E) can represent the strength of chemical bonds. It is generally evaluated by the amount of energy required to break the chemical bonds, which affects τ_f value. The smaller the bond valence, the smaller the bond energy required to recover the oxygen polyhedral deformation, leading to the decrease of τ_f value. The V_{ij} value of $Y_{2.95}R_{0.05}MgAl_3SiO_{12}$ ceramics is calculated by equations (7)-(8) [40,41]:

$$v_{ij} = exp\left\{\frac{R_{ij}-d_{ij}}{B}\right\} \quad (6)$$

$$V_{ij} = \sum_j^i v_{ij} \quad (7)$$

Where R_{ij} is the bond valence parameter, B is a constant (0.37 Å) and d_{ij} is the bond length. The calculated results for bond energy and bond valence are listed in Table S3 and Table S4 (Supporting Information). The average E, bond valence of $Al_{(Tet)}$-O and τ_f value are shown in Figure 7(a). It is observed that the τ_f value of $Y_{2.95}R_{0.05}MgAl_3SiO_{12}$ ceramics fluctuates from -28.6 to -38.7 ppm/°C, which is consistent with the changing trend of average E and bond valence. Figure 6(b) shows the average E of Y-O, $Al_{(Oct)}$-O and $Al_{(Tet)}$-O bond ($Al_{(Tet)}$-O (307.28 kJ/mol) > $Al_{(Oct)}$-O (224.10kJ/mol) > Y-O (218.47kJ/mol)), which indicates that the $Al_{(Tet)}$-O bond plays a major role in the temperature stability of $Y_{2.95}R_{0.05}MgAl_3SiO_{12}$ ceramics.

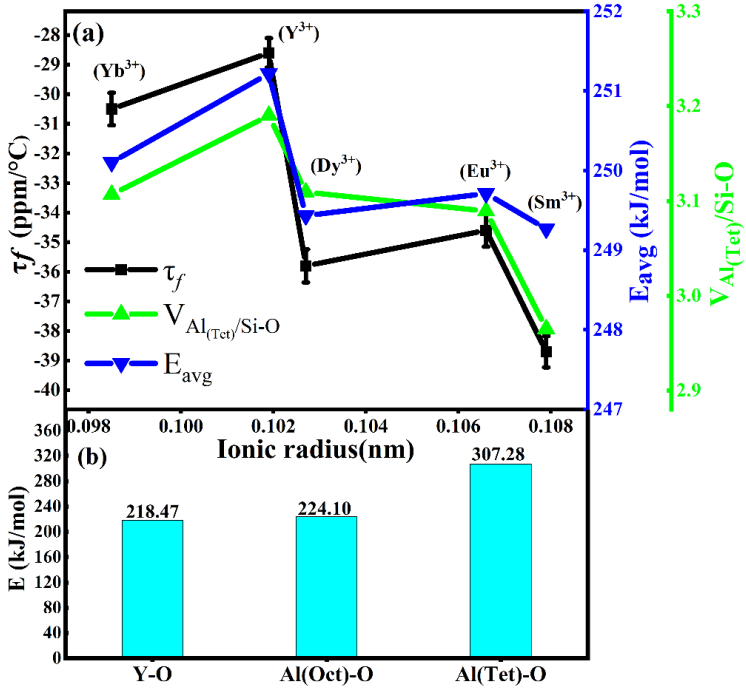

Figure 7. (a) The average E, bond valence of $V_{Al/Si-O}$ and τ_f value of $Y_{2.95}R_{0.05}MgAl_3SiO_{12}$ ceramic; (b) Average E of three types of bonds.

In order to further analyze the inherent microwave dielectric properties of $Y_{2.95}R_{0.05}MgAl_3SiO_{12}$ ceramics, the data of infrared reflectance spectrum is analyzed based on classical harmonic oscillator model:

$$R(\omega) = \left|\frac{\sqrt{\varepsilon^*(\omega)}-1}{\sqrt{\varepsilon^*(\omega)}+1}\right|^2 \quad (8)$$

$$\varepsilon^*(\omega) = \varepsilon'(\omega) - i\varepsilon''(\omega) = \varepsilon_\infty + \sum_{j=1}^{n} \frac{S_j}{\omega_j^2 - \omega^2 + i\omega\gamma_j} \quad (9)$$

The relevant parameters in the formula are described in detail in the previous literature [42,43]. The infrared reflectance spectrum can be well fitted with ten modes in Figure 8(a). Table S5 (Supporting Information) lists the relevant phonon parameters. For $Y_{2.95}Dy_{0.05}MgAl_3SiO_{12}$ ceramics, the theoretical ε_r (~8.55) at 10.86 GHz in Figure 8(b-c), less than the measured value (~9.68). The calculated $Q \times f$ value is 89,752 GHz (f = 10.86 GHz, Q = 1/tanδ and tanδ = 1.21 × 10^{-4}), which is greater than the measured value of 68,868 GHz. Differences between measurement values and the fitted infrared values are because of the extrinsic loss affected by all kinds of defects [44].

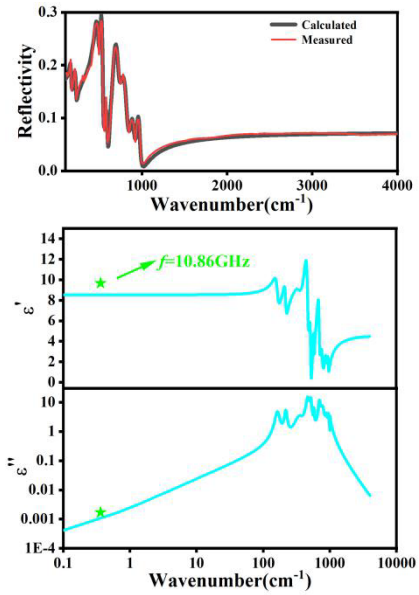

Figure 8. (a) Fitted and experimental infrared reflection spectrum of $Y_{2.95}Dy_{0.05}MgAl_3SiO_{12}$ ceramic and (b-c) fitted complex dielectric spectrum in the microwave region.

4. Conclusions

In this paper, the single-phase ceramics of $Y_{2.95}R_{0.05}MgAl_3SiO_{12}$ (R=Yb, Y, Dy, Eu, Sm) were successfully prepared using conventional ceramic technology. The relationship between the crystal structure, microstructure and microwave dielectric properties of $Y_{2.95}R_{0.05}MgAl_3SiO_{12}$ (R=Yb, Y, Dy, Eu, Sm) ceramic was analyzed by crystal structure refinement, scanning electron microscope (SEM), bond valence theory, P-V-L theory and infrared reflectance spectrum. The ε_r of $Y_{2.95}R_{0.05}MgAl_3SiO_{12}$ ceramics was mainly affected by the f_i of the Y-O bond. The τ_f value was mainly affected by the average E and bond valence of $Al_{(Tet)}$-O. In addition, infrared reflectance spectrum demonstrated that the calculated $Q \times f$ value was greater than the measured value, indicating the effect of extrinsic factors on the $Q \times f$ value. In particular, the microwave dielectric properties were obtained for $Y_{2.95}Dy_{0.05}MgAl_3SiO_{12}$ sintered at 1575 °C for 6 h, with ε_r = 9.68, $Q \times f$ = 68,866 GHz, and τ_f = -35.8 ppm/°C. The results show that $Y_{2.95}Dy_{0.05}MgAl_3SiO_{12}$ garnet ceramics have potential in 5G communication frequency band, such as dielectric substrate, microstrip patch antenna, etc.

Acknowledgments: This work was supported by the Natural Science Foundation of China (52161145401, and 51672063), the Guangdong Provincial Key Laboratory (2014B030301014) and the Construction of Basic Research Institutions from Shenzhen Science, Technology and Innovation Commission.

Declaration of Competing Interest: The authors declare that they have no known competing financial interests or personal relationships that could have appeared to influence the work reported in this paper.

References

[1] C. Du, D. Zhou, R.T. Li, H.T. Chen, G.H. Zhou, B. Tang, M.A. Darwish, S. Xia, Z. Xu. Fabrication of wideband low-profile dielectric patch antennas from temperature stable 0.65 CaTiO3-0.35 LaAlO3 microwave dielectric ceramic. A.D.V. Electron. Mater. 2022; 8: 2101414.

[2] G.X. Shen, W.Q. Che, W.J. Feng, Y.R. Shi, F. Xu, Q. Xue. Ultra-low-loss millimeter-wave LTCC Bandpass filters based on flexible design of lumped and distributed circuits. IEEE. T. Circuits-II. Pack. 2021; 68:1123-1127.

[3] Z.J. Wang, F. Pan, L.L. Liu, Q.F. Du, R.T. Tang, J. Ai, H. Zhang, Y. Chen. Enhanced microwave dielectric properties and sintering behaviors of Mg2SiO4-Li2TiO3-LiF ceramics by adding CaTiO3 for LTCC and GPS antenna applications. Crystals. 2022; 12:512.

[4] S.W. Wong, R.S. Chen, K. Wang, Z.N. Chen, Q.X. Chu. U-shape slots structure on substrate integrated waveguide for 40-GHz bandpass filter using LTCC technology. IEEE. T. Comp. Pack. Man. 2014; 5:128-134.

[5] F.F. Wu, D. Zhou, C. Du, S.K. Sun, L.X. Pang. Temperature stable $Sm(Nb_{1-x}V_x)O_4$ ($0.0<x<0.9$) microwave dielectric ceramics with ultra-low dielectric loss for dielectric resonator antenna applications. J. Mater. Chem. C. 2021; 9:9962.

[6] S.R. Xu, J. Jiang, Z.L. Cheng, X.Y. Chen, S.K. Sun, D.W. Wang, T.J. Zhang. Temperature stable, high-quality factor Li_2TiO_3-Li_4NbO_4 microwave dielectric ceramics. Crystals. 2021; 11:741.

[7] C. Du, M.S. Fu, D. Zhou, H.H. Guo, H.T. Chen, J. Zhang, J.P. Wang, S.F. Wang, H.W. Liu, W.F. Liu, L. Li, Z. Xu. Dielectric resonator antenna with $Y_3Al_5O_{12}$ transparent dielectric ceramics for 5G millimeter-wave applications. J. Am. Ceram. Soc. 2021; 104:4659-4668.

[8] H.F. Zhou, W.D. Sun, X.B. Liu. Microwave dielectric properties of $LiCa_3ZnV_3O_{12}$ and $NaCa_2Mg_2V_3O_{12}$ ceramics prepared by reaction-sintering. Ceram. Int. 2019; 45:2629-2634.

[9] Y. Tang, H. Li, J. Li, L. Fang. Relationship between Rattling Mg^{2+} ions and anomalous microwave dielectric behavior in $Ca_{3-x}Mg_{1+x}LiV_3O_{12}$ ceramics with garnet structure. J. Am. Ceram. Soc. 2021; 41:7697-7702.

[10] J. Chen, Y. Tang, H. Xiang, L. Fang. Microwave dielectric properties and infrared reflectivity spectra analysis of two novel low-firing $AgCa_2B_2V_3O_{12}$ (B=Mg, Zn) ceramics with garnet structure. J. Am. Ceram. Soc. 2018; 38:670-4676.

[11] Rakhi M, Subodh G. Crystal Structure and Microwave Dielectric Properties of $NaPb_2B_2V_3O_{12}$(B=Mg, Zn) Ceramics. J. Am. Ceram. Soc. 2018; 38:4962-4966.

[12] W. Jin, W. Yin, S. Yu, M. Tang, T. Xu, B. Kang, H. Huang. Microwave dielectric properties of pure YAG transparent ceramics. Mater. Lett. 2016; 173:47-49.

[13] J. Song, K. Song, J. Wei, H. Lin, J. Wu, J. Xu, W. Su, Z. Cheng. Ionic occupation, structures, and microwave dielectric properties of $Y_3MgAl_3SiO_{12}$ garnet-type ceramics. J. Am. Ceram. Soc. 2018; 101:244-251.

[14] X. Zhang, G. Fan, W. Lu, Y. Chen, X. Ruan. Effect of the spark plasma sintering parameters, LiF additive, and Nd dopant on the microwave dielectric and optical properties of transparent YAG ceramics. J. Eur. Ceram. Soc. 2018; 36:2767-2772.

[15] M. Zhou, B. Tang, Z. Xiong, X. Zhang, S. Zhang, Compounds. Effects of MgO doping on microwave dielectric properties of yttrium aluminum garnet ceramics. J. Alloys. Compd. 2021; 858:158139.

[16] M. Zhou, H. Chen, X. Zhang, B. Tang. Phase composition, microstructure, and microwave dielectric properties of non-stoichiometric yttrium aluminum garnet ceramics. J. Eur. Ceram. Soc. 2022; 42:472-477.

[17] J.C. Kim, M.H. Kim, J.B. Lim, S. Nahm, J.H. Paik, J.H. Kim. Synthesis and Microwave Dielectric Properties of $Re_3Ga_5O_{12}$ (Re: Nd, Sm, Eu, Dy, Yb, and Y) Ceramics. J. Am. Ceram. Soc. 2007; 90:641-644.

[18] J.C. Kim, M.H. Kim, S. Nahm, J.-H. Paik, J.-H. Kim, H.-J. Lee. Microwave dielectric properties of $Re_3Ga_5O_{12}$ (Re: Nd, Sm, Eu, Dy and Yb) ceramics and effect of TiO_2 on the microwave dielectric properties of $Sm_3Ga_5O_{12}$ ceramics. J. Eur. Ceram. Soc. 2007; 27:2865-2870.

[19] C.X. Su , L. Fang , L.Y. Ao , Q. B. Du. Correlation between crystal structure and microwave dielectric properties of two garnet-type ceramics in rare-earth-free gallates. J. Eur. Ceram. Soc. 2021; 41:1962-1968.

[20] C. Su, L.Y. Ao, Y. Zhai, Z.W. Zhang, Y. Tang. Novel low-permittivity microwave dielectric ceramics in garnet-type $Ca_4ZrGe_3O_{12}$. Materials Letters. 2020; 275:128149.

[21] Y.F. Zhai, Y. Tang, J. Lia, L. Duan, Structure. Raman spectra and properties of two low-ε_r microwave dielectric ceramics $Ca_3B_2Ge_3O_{12}$ (B = Al, Ga). Ceram. Int. 2020; 46:28710-28715.

[22] Y. Tang, Z.W. Zhang, J. Li, M.Y. Xua, Y.F. Zhai. $A_3Y_2Ge_3O_{12}$ (A = Ca, Mg): Two novel microwave dielectric ceramics with contrasting τ_f and $Q\times f$. J. Eur. Ceram. Soc. 2020; 40:3989-3995.

[23] J. Li, Y. Tang, Z.W. Zhang, W.S. Fang, L.Y. Ao, A.h. Yang, L.J. Liu, L. Fang. Two novel garnet $Sr_3B_2Ge_3O_{12}$ (B = Yb, Ho) microwave dielectric ceramics with low permittivity and high Q. J. Eur. Ceram. Soc. 2021; 41:1317-1323.

[24] H.R. Mei, L.B. Zhang, C.C. Li, Z.G. Rao, L.L. Shu. Compositional design, structure stability, and microwave dielectric properties in $Ca_3MgBGe_3O_{12}$ (B = Zr, Sn) garnet ceramics with tetravalent cations on B-site. Ceram. Int. 2022; 48:4658-4664.

[25] I. Kagomiya, Y. Matsuda, K. Kakimoto. Microwave dielectric properties of YAG ceramics. Ferroelectrics 2009; 387:1-6.

[26] S. Peng, C.G. Zhao, G.H. Huang, S.J. Wang, J.M. Xu, X.L. Li, S.Q. Yu. Crystal structure, sintering behavior and microwave dielectric properties of $Ca_xY_{3-x}Al_{5-x}Ti_xO_{12}$ ($0 \le x \le 2.0$) solid solution ceramics. J. Mater. Sci. Mater. Electron. 2018; 29:17047-17053.

[27] S.L. Jiang, T. C. Lu, J. Chen. Ab initio study the effects of Si and Mg dopants on point defects and Y diffusion in YAG. Comput. Mater. Sci. 2013; 69:261-266.

[28] G.F. Wu, M.T. Ma, A.H. Li, Crystal structure and microwave dielectric properties of Mg^{2+}-Si^{4+} co-modified yttrium aluminum garnet ceramics. J. Mater. Sci. Mater. Electron. 2022; 33:4712-4720.

[29] C. Li, J.L. Hou, Y.J. Ye. Lattice occupying sites and microwave dielectric properties of Mg^{2+}-Si^{4+} co-doped $Mg_xY_{3-x}Al_{5-x}Si_xO_{12}$ garnet typed ceramics. J. Mater. Sci. Mater. Electron. 2022; 33:2116-2124.

[30] Z.Y. Tan, K.X. Song, B. Liu, H.X. Lin, D.W. Wang. The effects of TiO_2 addition on microwave dielectric properties of $Y_3MgAl_3SiO_{12}$ ceramic for 5G application. Ceram. Int. 2020; 46:15665-15669.

[31] B.H. Toby. EXPGUI, a graphical user interface for GSAS. J. Appl. Crystallogr. 2001; 34:210-213.

[32] H.M. Rietveld. A profile refinement method for nuclear and magnetic structures. J. Appl. Crystallogr. 1969; 2:65-71.
[33] Y. J. Gu, X. B. Ding, W. Hu, et al. Effect of Mg/B ratio and Sr^{2+} substitution for Mg^{2+} on the sintering, phase composition and microwave dielectric properties of $Mg_3B_2O_6$ ceramics. Ceram. Int. 2020; 46:25888-25894.
[34] S. Wu, K.X. Song, P. Liu, H.X. Lin, F.F. Zhang, P. Zheng, H.B. Qin. Effect of TiO_2 doping on the structure and microwave dielectric properties of cordierite ceramics. Am. Ceram. Soc. 2015; 98:1842-1847.
[35] G. Mahan. Octupole modifications of the Clausius-Mossotti relation. Solid State Commun. 1980; 33:797-800.
[36] R.D. Shannon. Dielectric polarizabilities of ions in oxides and fluorides. J. Appl. Phy. 1993; 73:348-366.
[37] W. C. Lou, K. X. Song, F. Hussain, B. Liu, H. B. Bafrooei, H. X. Lin, W. T. Su, F. Shi, D. W. Wang. Bond characteristics and microwave dielectric properties of $(Li_{0.5}Ga_{0.5})^{2+}$ doped $Mg_2Al_4Si_5O_{18}$ ceramics. Ceram. Int. 2020; 46:28631-28638.
[38] M. Xiao, S.S. He, J. Lou, P. Zhang, Structure and microwave dielectric properties of $MgZr(Nb_{1-x}Sb_x)_2O_8$ ($0 \le x \le 0.1$) ceramics. J. Alloys Compd. 2019; 777:350-357.
[39] S.J. Penn, N.M. Alford, A. Templeton, X. Wang, M. Xu, M. Reece, K. Schrapel. Effect of porosity and grain size on the microwave dielectric properties of sintered alumina. J. Am. Ceram. Soc. 1997; 80:1885-1888.
[40] N. Brese, M. O'keeffe. Bond-valence parameters for solids. Acta Crystallogr. Sect. B Struct. Sci. 1991; 47:192-197.
[41] I.D. Brown, D. Altermatt. Bond-valence parameters obtained from a systematic analysis of the inorganic crystal structure database, Acta Crystallogr. Sect. B Struct. Sci. 1985; 41:244-247.
[42] C. Xing, J.Z. Li, J. Wang, H.L. Chen, H.Y. Qiao, X.Q. Yin, Q. Wang, Z.M. Qi, F. Shi. Internal relations between crystal structures and intrinsic properties of nonstoichiometric $Ba_{1+x}MoO_4$ ceramics. Inorg. Chem. 2018; 57:7121-7128.
[43] W.C. Lou, K.X. Song, F. Hussain. Microwave dielectric properties of $Mg_{1.8}R_{0.2}Al_4Si_5O_{18}$ (R= Mg, Ca, Sr, Ba, Mn, Co, Ni, Cu, Zn) cordierite ceramics and their application for 5G microstrip patch antenna. J. Eur. Ceram. Soc. 2022; 42:2254-2260.
[44] D. Guo, D. Zhou, W.B. Li, L.X. Pang, Y.Z. Dai, Z.M. Qi. Phase evolution, crystal structure, and microwave dielectric properties of water-insoluble (1-x)$LaNbO_4$-x$LaVO_4$($0 \leqslant x \leqslant 0.9$) ceramics, Inorg. Chem. 2017; 56:9321-9329.